JMEPEG (2011) 20:271–275
DOI: 10.1007/s11665-010-9684-3

1059-9495/$19.00

Inhibition of Corrosion of 3003 Aluminum Alloy in Ethylene Glycol-Water Solutions

Y. Liu and Y.F. Cheng

(Submitted March 9, 2010; in revised form April 13, 2010)

In this study, the inhibiting effects of four types of inhibitors, including gluconate, cinnamate, molybdate, and nitrate, on corrosion of a 3003 aluminum (Al) alloy were investigated in ethylene glycol-water solutions that simulate the automotive coolant by various electrochemical measurements. It was found that the tested inhibitors were effective to inhibit corrosion of 3003 Al alloy under both static and turbulent flow conditions. They all behave as anodic inhibitors, which inhibit the Al alloy corrosion by passivating Al alloy and decreasing its anodic current density. A turbulent flow of the solution decreases the corrosion resistance of Al alloy and the inhibiting effect of the inhibitors. The inhibiting effect of the inhibitors is ranked as: nitrate > cinnamate > gluconate > molybdate.

Keywords aluminum alloy, corrosion, ethylene glycol, inhibitor

1. Introduction

Previous studies (Ref 1-4) have demonstrated that aluminum (Al) alloy experiences serious flow-assisted corrosion (FAC) in the automotive cooling system, even in the coolant with a commercial inhibitor addition. It is realized that most of the currently available commercial coolants contain inhibitor that is not designed for Al alloy, but for stainless steels and copper alloys (Ref 5-7).

The inhibitor technologies against the Al corrosion have been tested in both inorganic salt solution, such as chromate, nitrate, nitrite, phosphate, sulfate, silicate, molybdate, dicarbonate and rare earth metal salts, and organic salts, such as gluconate, cinnamate, benzoate, alkyl amines, albumin, etc. (Ref 8-15). For example, Hawkins et al. (Ref 11) investigated the interaction of chromate species with Al specimens, and found that a rapid reduction of chromate species to thicken the passive film on the Al surface to resist corrosion. Na and Pyun (Ref 12) studied the effects of sulfate, nitrate, and phosphate on pitting initiation of pure Al in HCl-based solutions by potentiodynamic polarization and electrochemical noise measurements. It was found that the pit formation rate was increased by the addition of phosphate ions, but decreased gradually with an increasing sulfate or nitrate concentration. Silva et al. (Ref 13) studied the pitting corrosion of 2024-T351 and 7050-T7451 Al alloys in naturally aerated chloride solutions containing chromate, molybdate, and tungstate. They found that chromate-inhibited corrosion for the two alloys and molybdate for 7050 had a corrosion inhibiting effect, whereas tungstate promoted the pitting corrosion for both alloys.

Y. Liu and **Y.F. Cheng**, Department of Mechanical and Manufacturing Engineering, University of Calgary, Calgary, AB T2N 1N4, Canada. Contact e-mail: fcheng@ucalgary.ca.

To date, most of work about the inhibition of the Al alloy corrosion has been performed in static aqueous solutions which are quite different from the flowing coolant. It has been demonstrated (Ref 16, 17) that the fluid hydrodynamic condition would affect significantly the inhibiting performance. There has been so far limited work performed to test inhibitors for Al alloy corrosion in ethylene glycol-water solutions (Ref 18, 19).

In this work, the inhibiting effect of five inhibitors, including sodium gluconate, sodium cinnamate, sodium molybdate, sodium chromate, and sodium nitrate, on electrochemical corrosion of a 3003 Al alloy in ethylene glycol-water solutions was investigated through a rotating cylinder electrode (RCE) technique simulating the hydrodynamic condition of the automotive cooling system. Various electrochemical measurements, including corrosion potential, linear polarization resistance, cyclic polarization scanning and electrochemical impedance spectroscopy (EIS), were conducted to study the corrosion behavior of the Al alloy electrode in the presence and absence of inhibitors. The inhibiting effects under both static and turbulent flow conditions were tested and compared. Effect of the hydrodynamic condition on the inhibiting performance was discussed.

2. Experimental Procedure

2.1 Electrode and Solution

Test specimens were cut from a round bar of 3003 Al alloy supplied by Dana Canada Corporation, with the chemical composition (wt.%): Cu 0.20, Fe 0.70, Si 0.60, Mn 1.50, Mg 0.05, Cr 0.05, Zn 0.10, Ti 0.05, and Al balance. The electrode was machined and embedded in an epoxy resin manufactured by LECO, leaving a working area of 1 cm^2. The RCE of ∅16.5 mm × 7 mm had a working area of 3.63 cm^2. The working surface of the electrodes was ground with 800 and 1200 grit silicon carbide papers, polished with a 1-μm alumina paste, cleaned by deionized water and then dried in air.

The base solution was a mixture of 50% (v/v) ethylene glycol + 50% deionized water + 100 ppm NaCl, simulating the automotive coolant and the potential chloride contamination from the use of water. To investigate the inhibiting effect, 1% (w/w) sodium gluconate, sodium cinnamate, sodium molybdate and sodium nitrate were added in the base solution, respectively. The pH of the solution was about 6.47. All solutions were made from analytic grade reagents and ultra-pure deionized water (18 MΩ cm in resistivity).

2.2 Hydrodynamic Simulation

During test, the rotating speed of RCE was set at 3000 rpm. The Reynolds number (*Re*) was determined by the geometry of the electrode, fluid flow velocity, and kinematic viscosity of the solution by (Ref 20):

$$\mathrm{Re} = \frac{2\omega r^2}{\nu} \quad \text{(for RCE)}, \qquad \text{(Eq 1)}$$

where ω is the angular rotating velocity of RCE, r is the radius of RCE, and ν is kinematic viscosity of the solution (2.03×10^{-6} m^2 s^{-1}). At a rotating speed of 3000 rpm, *Re* was approximately equal to 20,000, representing a turbulent flow.

2.3 Electrochemical Measurement

Electrochemical measurements were conducted on a three-electrode cell, where 3003 Al alloy RCE was used as working electrode (WE), a saturated calomel electrode (SCE) as reference electrode (RE), and a Pt wire as counter electrode (CE), using a Solartron 1280c electrochemical system. The IR drop compensation mode of the instrument was set at "ON" with an input value around 6,000 Ω, which was estimated through the EIS measurement.

Prior to electrochemical measurement, the Al alloy WE was immersed in the static solution or at a rotating speed of 3,000 rpm for 3 days. Linear polarization resistance measurement was then performed at the potential range of $E_{corr} \pm 25$ mV, with a potential sweep rate of 0.166 mV/s. The values of polarization resistance, corrosion current density, and corrosion potential were fitted through a PowerCORR analytical software.

The cyclic polarization scan was performed at a positive direction with a potential sweep rate of 1 mV/s. The scan direction was reversed when the anodic current density reached 100 μA/cm^2.

The EIS were measured on the electrode that was at corrosion potential, with a sinusoidal potential excitation of 20 mV (peak-to-peak) in the frequency range from 10^5 to 10^{-3} Hz.

All the tests were performed at a room temperature (about 20 °C) and open to air.

3. Results

3.1 EIS Measurement

Figure 1 shows the Nyquist diagrams measured on 3003 Al alloy electrode immersed in static base solution containing 1%(w/w) of various inhibitors. It is seen that all the impedance plots were featured with a semicircle over the whole frequency range. Upon addition of inhibitor, the size of the semicircle increased. In particular, there was the largest semicircle measured in the cinnamate-containing solution.

Figure 2 shows the Nyquist diagrams measured on 3003 Al alloy RCE with a rotating speed of 3000 rpm immersed in the base solution containing 1%(w/w) of various inhibitors. It is seen that, when the solution contained inhibitor, the size of the semicircle increased. There was the largest semicircle measured in cinnamate-containing solution. Furthermore, there was the identical feature of the impedance plots to those measured in the static solution, but with a smaller size. However, it is worthy pointing out that it is hard to judge if the size of the largest semicircle also decreased upon solution-flowing from Fig. 1 and 2.

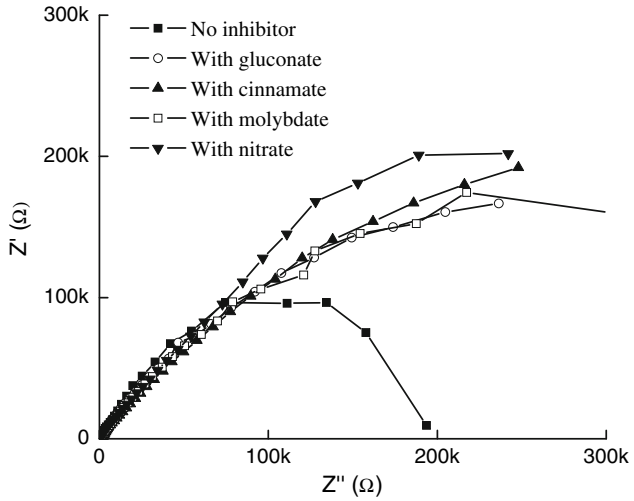

Fig. 1 Nyquist diagrams measured on 3003 Al alloy electrode immersed in static base solution containing 1%(w/w) of various inhibitors

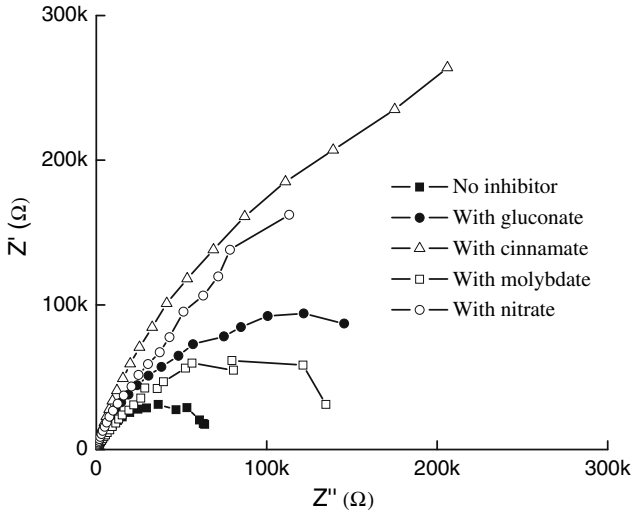

Fig. 2 Nyquist diagrams measured on 3003 Al alloy RCE with a rotating speed of 3000 rpm immersed in the base solution containing 1%(w/w) of various inhibitors

3.2 Anodic Cyclic Polarization Curves Measurement

Figure 3 shows the anodic cyclic polarization curves of 3003 Al alloy electrode in static base solutions containing 1%(w/w) of various inhibitors. It is seen that the addition of inhibitors decreased the anodic current density, following the order of gluconate > molybdate > cinnamate > nitrate.

Figure 4 shows the anodic cyclic polarization curves of 3003 Al alloy RCE electrode at a rotating speed of 3000 rpm in the base solution containing 1%(w/w) of various inhibitors. It is seen that there was the approximately identical feature of the anodic polarization curves to those measured under static condition. There was the smallest passive potential region and the highest passive current density measured in the absence of inhibitor. The addition of inhibitors would widen the passive range and decrease the anodic current density. In particular, the inhibiting effect was most apparent in nitrate-containing solution.

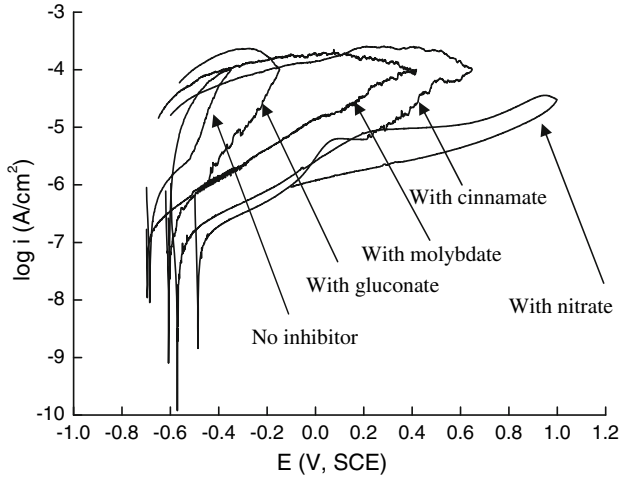

Fig. 3 Anodic cyclic polarization curves of 3003 Al alloy electrode in static base solutions containing 1%(w/w) of various inhibitors

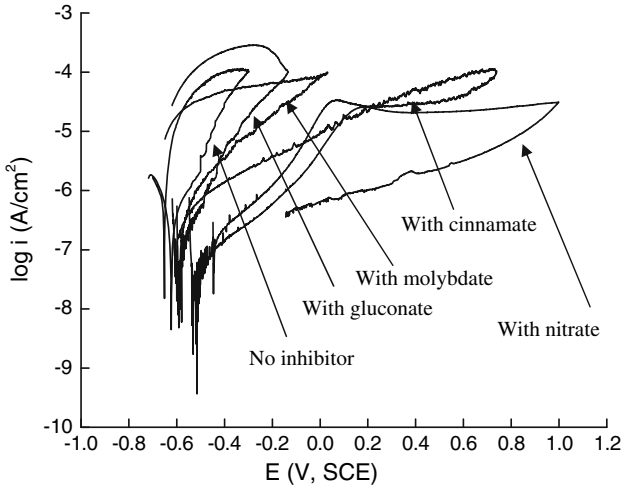

Fig. 4 Anodic cyclic polarization curves of 3003 Al alloy RCE electrode at a rotating speed of 3000 rpm in the base solution containing 1%(w/w) of various inhibitors

3.3 Linear Polarization Resistance Measurement

Figure 5 shows the linear polarization resistances measured on 3003 Al alloy RCE electrode rotating at 3000 rpm in the base solution without and with 1%(w/w) of various inhibitors. According to Stern and Geary model (Ref 21, 22), the polarization resistance (R_p) is obtained from the fitting slope (dE/di) of the linear relationship between potential and current density:

$$R_p = \left[\frac{\Delta E}{\Delta i}\right]_{\Delta E \to 0} \quad \text{(Eq 2)}$$

The corrosion current density (i_{corr}) was calculated by:

$$i_{corr} = \frac{B}{R_p}, \quad \text{(Eq 3)}$$

where B is a proportionality constant which is usually taken as 26 mV (Ref 23).

The fitting values of R_p, i_{corr}, and E_{corr} are listed in Table 1. It is seen that there was the lowest i_{corr} in nitrate- and cinnamate-containing solutions.

3.4 Corrosion Potential Measurement

Figure 6 shows the corrosion potential measurements of 3003 Al alloy RCE electrode at a rotating speed of 3000 rpm in the various solutions. It is seen that the addition of inhibitor shifted E_{corr} of Al alloy positively.

4. Discussion

The capacitive semicircle in Nyquist diagram is typical associated with the interfacial charge-transfer reaction, with the diameter of the semicircle relating to the charge-transfer resistance (Ref 24, 25). The present study shows that, under both static and flowing conditions, the size of the semicircles measured in the presence of inhibitors is larger than that measured without inhibitor (Fig. 1 and 2), indicating the effective inhibition of the inhibitors to corrosion of 3003 Al alloy in ethylene glycol-water solutions.

The inhibiting effect of the inhibitors is also confirmed by the anodic polarization curve measurements (Fig. 3 and 4). The decreasing current density upon the addition of inhibitors shows that the dissolutive activity of the electrode decreases. Particularly, cinnamate and nitrate have the best inhibiting effect, as indicated by the decreasing current density and the linear polarization resistance measurements (Fig. 5 and Table 1), where the addition of the two inhibitors result in the lowest i_{corr}.

Furthermore, all inhibitors shift E_{corr} of Al alloy to the positive direction (Fig. 6). Thus, the inhibitors behave as anodic inhibitors, which inhibit primarily the anodic reaction process (Ref 10). As shown in Fig. 3 and 4, an addition of the inhibitors would passivate the Al alloy, and decrease the anodic current density.

It has been acknowledged (Ref 3, 8) that a laminar flow of the solution could accelerate the mass transport of oxygen toward the electrode surface to contribute the formation of passive film, resulting in an increasing corrosion resistance. However, the turbulent flow could weaken, damage, and even remove completely the passive film, decreasing the corrosion resistance (Ref 9). In this study, the RCE rotating speed of 3000 rpm results

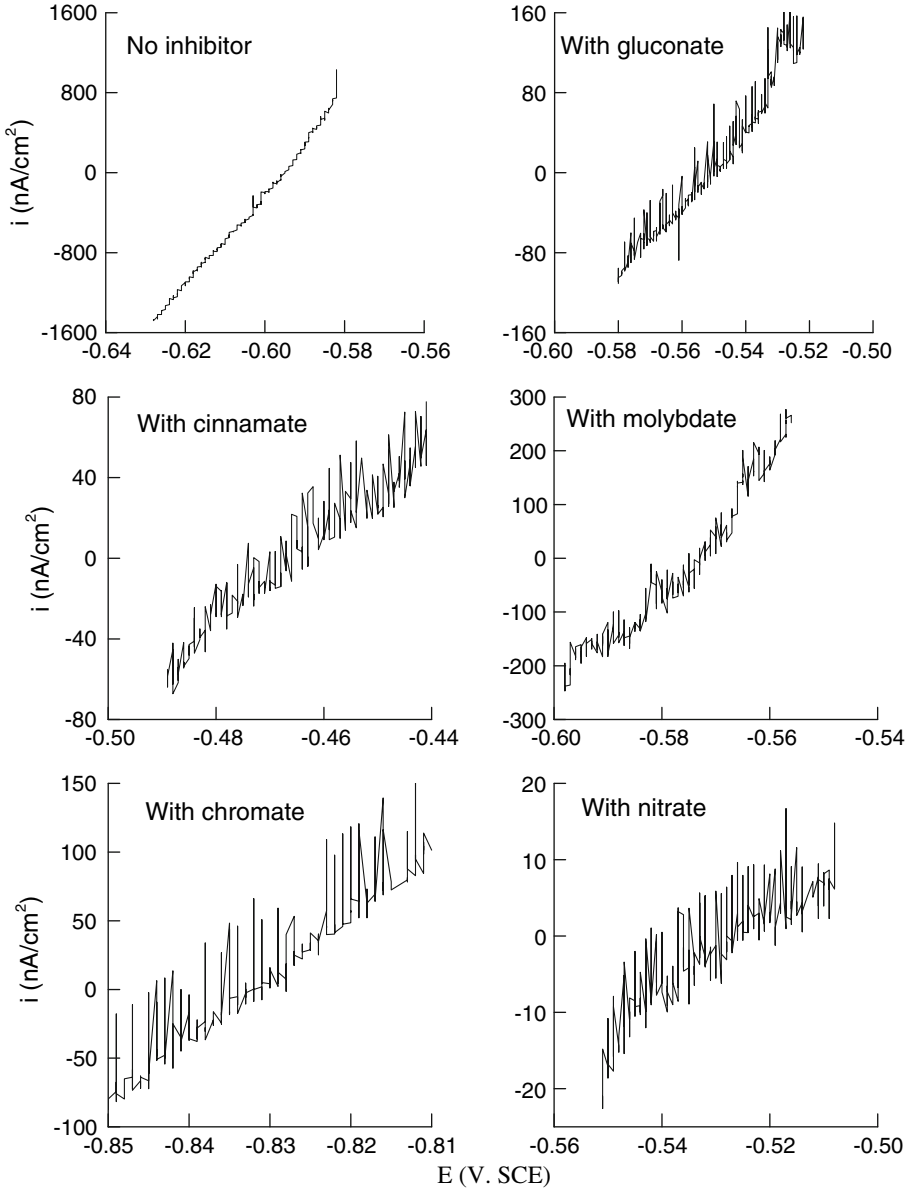

Fig. 5 Linear polarization resistances measured on 3003 Al alloy RCE electrode rotating at 3000 rpm in the base solution without and with 1%(w/w) of various inhibitors

Table 1 Fitting values of polarization resistance, R_p, corrosion current density, i_{corr}, and corrosion potential, E_{corr}, for 3003 Al alloy RCE electrode at a rotating speed of 3000 rpm in the various solutions

Inhibitor	R_p ($\times 10^5$), Ω cm^2	i_{corr}, nA/cm^2	E_{corr}, V, SCE
Ni	0.21	1220	−0.6
Gluconate	11.5	22.6	−0.55
Cinnamate	14.3	18.2	−0.47
Molybdate	2.77	94.2	−0.58
Nitrate	22.7	11.4	−0.53

in a *Re* of about 20,000, which represents a turbulent flowing fluid. Therefore, the charge-transfer resistance obtained in EIS plots, i.e., the size of the semicircle, under the flowing condition is lower than those measured under the static condition.

The present study demonstrates that the tested inhibitors work well to resist corrosion of Al alloy in the turbulent fluid system. Compared to the electrochemical measurements under the static condition, both charge-transfer resistance and corrosion current density obtained in the presence of inhibitor favor the inhibiting effect on the Al alloy corrosion. According to i_{corr} determined from the linear polarization measurements, the inhibiting effect is ranked as: nitrate > cinnamate > gluconate > molybdate.

5. Conclusions

Gluconate, molybdate, cinnamate, and nitrate are effective to inhibit corrosion of 3003 Al alloy in ethylene glycol-water solutions under both static and turbulent flow conditions.

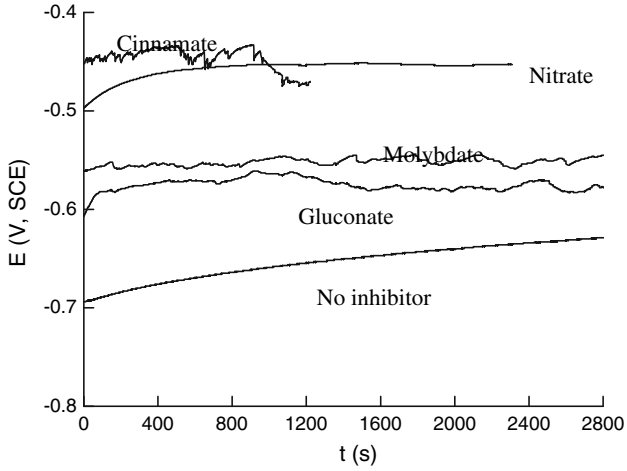

Fig. 6 Corrosion potential measurements of 3003 Al alloy RCE electrode at a rotating speed of 3000 rpm in the various solutions

They all behave as anodic inhibitors, which inhibit the Al alloy corrosion by passivating Al alloy and decreasing its anodic current density. The turbulent flow of the solution decreases the corrosion resistance of Al alloy and the inhibiting effect of the inhibitors. The inhibiting effect of the tested inhibitors are ranked as nitrate > cinnamate > gluconate > molybdate.

Acknowledgments

This work was supported by Canada Research Chairs Program, Natural Science and Engineering Research Council of Canada (NSERC) and Dana Canada Corporation.

References

1. L.Y. Xu and Y.F. Cheng, Electrochemical Characterization and CFD Simulation of Flow-Assisted Corrosion of Aluminum Alloy in Ethylene Glycol-Water Solution, *Corros. Sci.*, 2008, **50**, p 2094–2100
2. G.A. Zhang, L.Y. Xu, and Y.F. Cheng, Mechanistic Aspects of Electrochemical Corrosion of Aluminum Alloy in Ethylene Glycol-Water Solution, *Electrochim. Acta*, 2008, **53**, p 8245–8252
3. Y. Liu and Y.F. Cheng, Cathodic Reaction Kinetics and Its Implication on Flow-Assisted Corrosion of Aluminum Alloy in Aqueous Ethylene Glycol Solution, *J. Appl. Electrochem.*, 2009, **39**, p 1267–1272
4. L.Y. Xu and Y.F. Cheng, Effect of Fluid Hydrodynamics on Flow-Assisted Corrosion of Aluminum Alloy in Ethylene Glycol-Water Solution Studied by a Microelectrode Technique, *Corros. Sci.*, 2009, **51**, p 2330–2335
5. Institution of Mechanical Engineers, *Corrosion of Motor Vehicles*, Mechanical Engineering Publications Limited, London, UK, 1976
6. C.C. Nathan, *Corrosion Inhibitors*, NACE, Houston, TX, 1981
7. J.C. Cessna, Problems in the Use of Corrosion Inhibitors in Automobile Engine Cooling Systems, *Mater. Prot.*, 1964, **3**, p 37–41
8. J.R. Davis, *Corrosion of Aluminum and Aluminum Alloys*, ASM International, Materials Park, 2000
9. S.B. Twiss and J.D. Guttenplan, Corrosion Testing of Aluminum. Part 2—Development of a Corrosion Inhibitor, *Corrosion*, 1956, **12**, p 311t–316t
10. E.W. Flick, *Corrosion Inhibitors*, Noyes Publications, Park Ridge, NJ, 1993
11. J.K. Hawkins, H.S. Isaacs, S.M. Heald, J. Tranguada, and G.C. Wood, Non-Chromate Corrosion Inhibitors for Aluminum Alloys, *Corros. Sci.*, 1987, **27**, p 391–399
12. K.H. Na and S.I. Pyun, Effects of Sulphate, Nitrate and Phosphate on Pit Initiation of Pure Aluminum in HCl-Based Solution, *Corros. Sci.*, 2007, **49**, p 2663–2675
13. J.W.J. Silva, E.N. Codaro, R.Z. Nakazato, and L.R.O. Hein, Influence of Chromate, Molybdate and Tungstate on Pit Formation in Chloride Medium, *Appl. Surf. Sci.*, 2005, **252**, p 1117–1122
14. K.C. Emregul and A.A. Aksut, The Effect of Sodium Molybdate on the Pitting Corrosion of Aluminum, *Corros. Sci.*, 2003, **45**, p 2415–2433
15. J.G.N. Thomas, G. Treacy, and W.M. Carrol, Corrosion of Aluminum Alloys in Chlor-Alkali Environments, *Corros. Sci.*, 1994, **36**, p 11–14
16. H. Ashassi-Sorkhabi and E. Asghari, Effect of Hydrodynamic Conditions on the Inhibition Performance of L-Methionine as a "Green" Inhibitor, *Electrochim. Acta*, 2008, **54**, p 162–167
17. P. Bommersbach, C. Alemany-Dumont, J. Millet, and B. Normand, Hydrodynamic Effect on the Behaviour of a Corrosion Inhibitor Film: Characterization by Electrochemical Impedance Spectroscopy, *Electrochim. Acta*, 2008, **51**, p 4011–4018
18. B.A. Abd-El-Nabey, N. Khalil, and E. Khamis, The Acid Corrosion of Aluminum in Water-Organic Solvent Mixtures, *Corros. Sci.*, 1985, **25**, p 225–232
19. J. Zaharieva, M. Milanova, M. Mitov, L. Lutov, S. Manev, and D. Todorovsky, Corrosion of Aluminium and Aluminium Alloy in Ethylene Glycol-Water Mixtures, *J. Alloys Comp.*, 2009, **470**, p 397–403
20. G. Kear, B.D. Barker, K.R. Stokes, and F.C. Walsh, Electrochemistry of Non-Aged Copper-Nickel (UNS C70610) in Fully Developed Fluid Flows. Part 1: Cathodic and Anodic Characteristics, *Electrochim. Acta*, 2007, **52**(5), p 1889–1898
21. M. Stern and A.L. Geary, Electrochemical Polarization, A Theoretical Analysis of the Shape of the Polarization Curves, *J. Electrochem. Soc.*, 1957, **104**, p 56–63
22. M. Stern and A.L. Geary, The Mechanism of Passivating Type Inhibitors, *J. Electrochem. Soc.*, 1958, **105**, p 638–647
23. R.G. Kelly, J.R. Scully, D.W. Shoesmith, and R.G. Buchheit, *Electrochemical Techniques in Corrosion Science and Engineering*, Marcel Dekker Inc., New York, NY, 2003
24. E. Barsoukov and J.R. Macdonald, *Impedance Spectroscopy Theory, Experiment, and Applications*, Wiley & Sons Inc., NJ, 2005
25. J.R. Scully, D.C. Silverman, and M.W. Kendig, *Electrochemical Impedance: Analysis and Interpretation*, ASTM, Philadelphia, 1993